THE NEW ZEALAND CONCRETE INDUSTRY
CONFERENCE 2015
Rotorua Convention Centre 8-10 October

# PREDICTING THE SHEAR STRENGTH OF CONCRETE STRUCTURES

M.P.COLLINS; E.C.BENTZ; P.T.QUACH; A.W.FISHER; G.T. PROESTOS

Department of Civil Engineering, University of Toronto, Canada

## SUMMARY

Because many shear design techniques rely on empirical equations derived from rather small scale experiments there is concern that these traditional techniques may give unconservative estimates of shear strength when applied to very large reinforced concrete members with small amounts of shear reinforcement. This paper will describe the loading to failure of a strip from a four metre thick slab and the associated challenge issued to engineers to predict the shear response. Also discussed is the shear response of heavily reinforced coupling beams for shear walls.

## INTRODUCTION

Deficiencies in the shear design of concrete structure are inherently more dangerous than deficiencies in flexural design because shear failures can occur with no prior warning and with no possibility for redistribution of internal forces. While accurate assessment of the shear capacity of a reinforced concrete structure is critically important for public safety, the traditional techniques available for this task are open to dispute. For determining flexural capacity engineers can use the simple, accurate, general and internationally accepted “plane sections theory”. However, for finding shear strength engineers typically rely on restricted empirical equations whose applicability and accuracy are sometimes very questionable.

Mat or raft foundations for high rise buildings were in the past typically constructed to be thick enough not to need shear reinforcement according to traditional shear design procedures (e.g. ACI 318 2014). In a departure from this tradition the 5.33 m thick mat foundation of the 73 storey Wilshire Grand building (Nieblas 2014) now under construction in Los Angeles does contain significant amounts of shear reinforcement, see Figure 1. This reinforcement was specified partly to alleviate concerns with the so called “size effect” in shear which is based on the observation that as depth of reinforced concrete members without shear reinforcement increase the shear stress to cause failure decreases(Collins and Kuchma 1999). The size effect in shear is predicted by the Modified Compression Field Theory (MCFT Vecchio and Collins 1986) which forms the basis of the shear provisions of the AASHTO-LRFD “Bridge Design Specifications”, the Canadian Standard “Design of Concrete Structures”, CSA A23.3-14 and the fib “Model Code 2010”. These procedures predict that the shear capacity of a slab such as that shown in Figure 1 in regions without shear reinforcement can be less than one third of the shear strength predicted by ACI. To verify these predictions it was decided to fabricate and test to failure a strip from a four metre thick slab, see Figure 2.

Figure 1. Reinforcement in mat foundation of Wilshire Grand

Figure 2. Strip from four metre thick slab and 300 mm deep traditional size shear specimen

## MODIFIED COMPRESSION FIELD THEORY (MCFT)

The shear design procedures developed at the University of Toronto over the last 40 years (Collins 1978) by studying reinforced concrete elements loaded in pure shear will be briefly summarized before discussing the current experiments. Figure 3 shows the five equilibrium equations, five geometric conditions and five stress-strain relationships of the MCFT. In the upper part of the figure the equations deal with average stresses, average strains and the relationships between average stresses and average strains. Average stresses (e.g. $f_{sx}$) and average strains (e.g. $\varepsilon_x$) correspond to stresses and strains averaged out over lengths long enough to damp out the local variations that occur at cracks and between cracks. The bottom five relationships in the figure are concerned with stresses at a crack (e.g. $f_{sxcr}$), the crack width and the maximum shear stress that can be transmitted across the crack. The term $v_{ci}$ stands for shear stress transmitted across the crack interface. The average stress-average strain relationships for cracked concrete given by Eq. 13 and Eq. 14 in Fig. 3 are the result of experiments on reinforced concrete elements tested in pure shear. For higher strength concretes more accurate results are obtained if the 170 coefficient in Eq. 14 of Fig. 3 is replaced by $3f_c'$ where $f_c'$ is in MPa. The relationship used for determining the ability of the crack surfaces to transmit the interface shear stresses, Eq. 15 in Fig. 3, was derived from the aggregate interlock experiments of Walraven (1981). Note that this shear stress limit is a function of the crack width, $w$, the maximum aggregate size, $a_g$, and the concrete cylinder strength, $f_c'$.

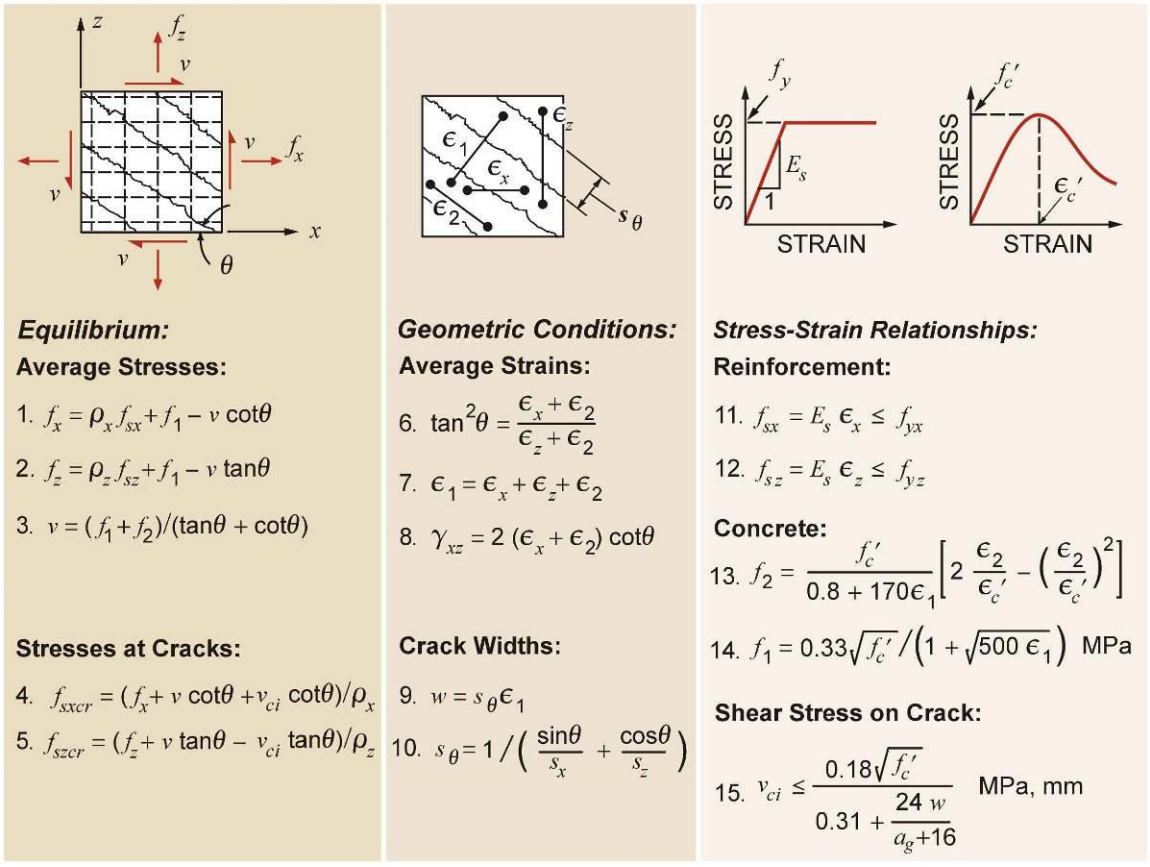


Figure 3: The modified compression field theory (MCFT)

The 15 equations of the MCFT can be conveniently solved using program Membrane available on the web (Bentz 2014).To use the MCFT to predict the load-deformation response of a reinforced concrete beam such as that shown in Fig. 4, the beam could be represented as a two dimensional grid of elements with the response of each element being predicted by the MCFT. This is the basis of non-linear finite element programs such as VecTor2 (Vecchio 2014).

If such a program is used to analyze the beam it will be found that in zones extending for a distance of about d away from the point loads and the reactions, there will be significant vertical compressive stresses in the concrete. These clamping stresses will enhance the shear strength of the elements in these zones making it probable that the shear failure will occur outside of these zones. For beams with short shear spans the zones with significant clamping stresses will overlap and the shear strength of the beam will be considerably increased. In these "disturbed regions" the shear stress distribution over the depth of the beam is influenced by the distribution of the clamping stresses and near the loads and reactions, plane sections do not remain plane.

Outside of the disturbed regions it is appropriate to assume that plane sections remain plane and that the clamping stresses are negligible. With these two assumptions a beam cross-section can be modeled as a stack of biaxially stressed elements with the response of each element being predicted by the MCFT. This is the basis of program Response (Bentz 2015) which can be used to predict the shear stress distribution over the depth of the beam and the complete load-deformation response of concrete sections subjected to shear, flexure and axial load, see Fig. 4.

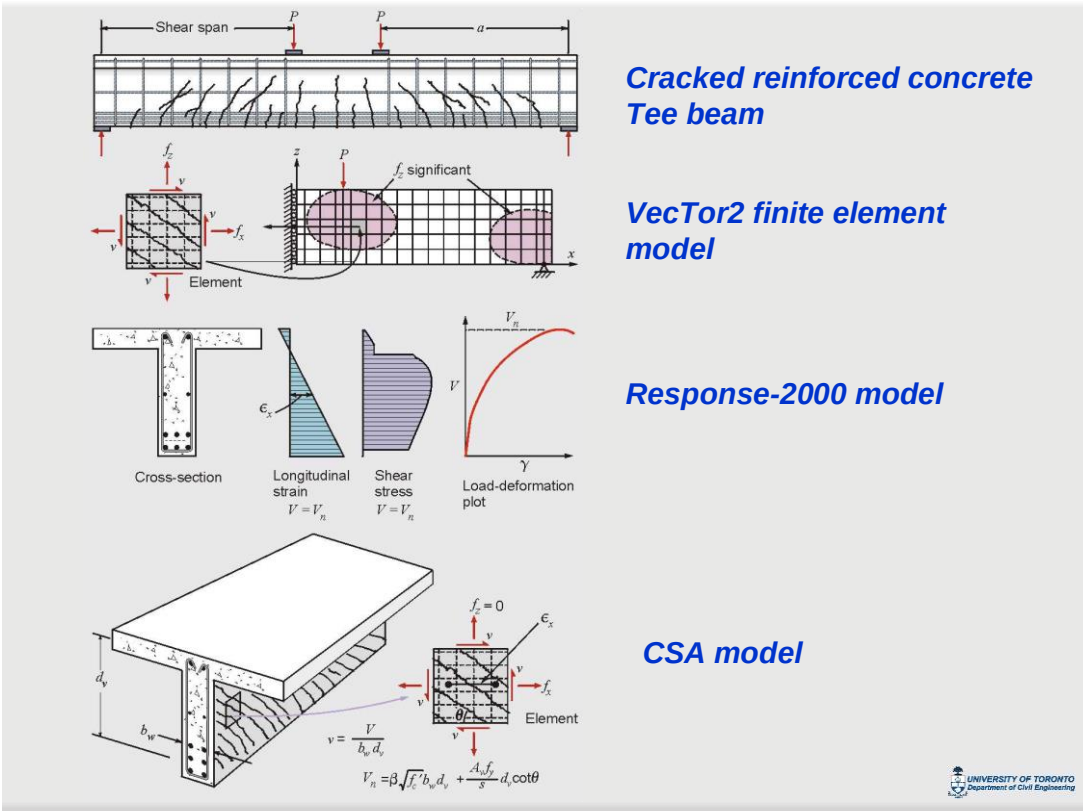


Figure 4: Levels of Approximation in MCFT Analyses

If only the shear strength of a beam cross-section is required, then the web of the beam can be approximated by just one biaxial element located at mid-depth and the shear stress on the element can be assumed to be $V/(b_w d_v)$ where $b_w$ is the web width and $d_v$ is the flexural lever arm which can be taken as $0.9d$. The longitudinal strain, $\varepsilon_x$, at mid-depth of the beam can be found from the calculated strain in the longitudinal flexural reinforcement and the assumption that plane sections remain plane. For a given value of $\varepsilon_x$ the failure shear stress can then be calculated from the MCFT as the sum of two terms, $V_c$ and $V_s$, see Fig. 4. This simplified MCFT sectional design model for shear (Bentz and Collins 2006) is the method used in the Canadian code CSA A23.3-14 (2014).

The unfactored shear strength, $V_n$, of a section as calculated by the Canadian code can be determined from the following equations where the unfactored failure shear stress $v_n$ is defined as $V_n/(b_w d_v)$ where $d_v$ can be taken as $0.9d$:

$$v_n = \beta\sqrt{f'_c} + \rho_z f_y \cot\theta \quad \leq 0.25 f'_c \tag{1}$$

The aggregate interlock parameter β primarily depends on the width of the cracks and size of the aggregate $a_g$. As crack width depends on both the average tensile strain in the cracked concrete and the crack spacing it is not surprising that the expression for $\beta$ derived from the MCFT has a strain term and a crack spacing term. The equation is

$$\beta = \frac{0.4}{1+1500\varepsilon_x} \cdot \frac{1300}{1000+s_{xe}} \tag{2}$$

The longitudinal strain at mid-depth, $\varepsilon_x$, can be conservatively taken as one half of the tensile strain in the flexural tensile reinforcement. Allowing for the tension in the longitudinal reinforcement caused by the shear and assuming that there is no axial load or prestressing gives

$$\varepsilon_x = v_n \frac{1+M/(V\cdot d_v)}{2E_s\rho_\lambda} \tag{3}$$

where M/V is the ratio of bending moment to shear at the section being considered and $\rho_\ell$ is the geometric ratio of the area of longitudinal flexural tension reinforcement to the shear area. That is: $\rho_\ell = A_s/(b_w d_v)$.

If the member contains more than the specified minimum amount of shear reinforcement (i.e. $\rho_z f_y \geq 0.06\sqrt{f'_c}$) then it can be assumed that the crack spacing will be well controlled and hence $s_{xe}$ can be taken as 300 mm which reduces the crack spacing term in Eq. (2) to unity. If the member contains only concentrated longitudinal reinforcement then the spacing of vertical cracks near mid-depth of the member, $s_x$, is assumed to be equal to $0.9d$. To allow for the influence of aggregate size the effective crack spacing, derived from Eq.(15) in Fig.3, is taken as:

$$s_{xe} = \frac{35 s_x}{15+a_g} \quad \geq 0.85 s_x \tag{4}$$

For high strength concrete the cracks will go through the aggregate rather than around the aggregate particles leading to smoother crack surfaces with less aggregate interlock capacity. To account for this, if $f_c'$ exceeds 70 MPa the term $a_g$ in Eq. (4) is taken as zero. As $f_c'$ goes from 60 MPa to 70 MPa, $a_g$ is linearly reduced to zero. As an additional allowance for the low aggregate interlock capacity of high strength concrete the term $\sqrt{f'_c}$ in Eq. (1) is not allowed to exceed 8 MPa.

The MCFT predicts that the angle of the principal compressive stress, $\theta$, at shear failure for members with shear reinforcement depends primarily upon the longitudinal strain, $\varepsilon_x$ as:

$$\theta = 29^\circ + 7000\varepsilon_x \tag{5}$$

## DESIGN OF THE SLAB STRIP SPECIMEN

The large slab strip specimen, called PLS4000, was designed so it would fail first in the 12 m long east shear span not containing shear reinforcement, see Fig. 5 . With a simple span of 19 m the specimen was loaded by its own substantial self-weight, 24.4 kN/m, and an off-centre point load. The nine high strength steel bars acting as flexural tension reinforcement had a total yield force of 3610 kN giving the section a flexural capacity of about 13100 kNm. Thus the magnitude of the point load to cause flexural failure of the specimen was predicted to be 2730 kN.

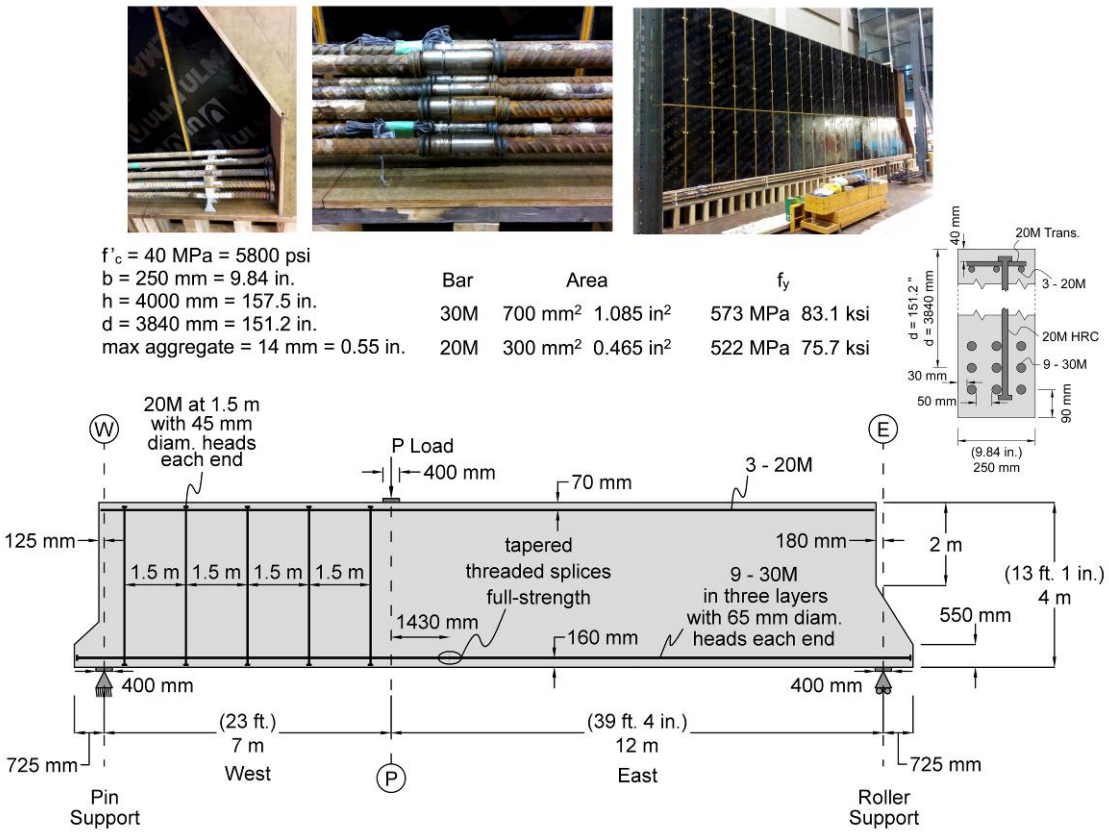


Figure 5. Details of the 4 m thick slab strip specimen PLS4000

Figure 6 summarizes the calculations involved in predicting the values of the point load, P, which will cause shear failure of PLS4000 and of the small companion specimen PLS300. Equation (6) given below is the SI unit version of the "basic expression for $V_c$" developed in 1962 (ACI-ASCE 326) and still used in ACI 318-14 (2014). The expression was derived based on the correct assumption that the failure shear stress will decrease as the stress in the flexural tension reinforcement increases and by determining the coefficients based on empirically fitting to the failure shears from 194 relatively small beams.

$$V_c = \left( 0.158\sqrt{f_c'} + 17.2\rho_w \frac{Vd}{M} \right) b_w d \qquad (6)$$

For PLS4000 three sections along the east shear span are checked in Fig. 6 (a): Section 1, d from the face of the support; Section 2 half-way along the shear span; and Section 3, d from the face of the load. As load P is increased the moments and shears at these three sections increase from the self-weight values to the predicted failure values. It can be seen that Section 1 has the smallest increment of shear to cause failure giving an ACI prediction for the

magnitude of P at shear failure of 2530 kN which is 93% of the value of P to cause a flexural failure. For the small specimen self-weight is negligible and the ACI prediction of the value of P to cause failure is 102.4 kN, see Fig. 6(b).

Equation (7) given below is the directly comparable MCFT equation to the ACI Eq. (6):

$$V_c = \frac{0.4}{(1+1500\varepsilon_x)}\frac{1300}{(1000+s_{xe})}\sqrt{f'_c}\cdot b_w d_v \qquad (7)$$

The resulting shear-moment interaction diagrams shown in Fig. 6 were calculated by choosing values of $\varepsilon_x$ calculating V from Eq. (7) and then finding the corresponding M from Eq. (3). The point load value predicted to cause a shear failure of the large slab, PLS4000, is 662 kN which is only 26% of the ACI predicted shear failure value of P while for the small specimen, PLS300, the predicted failure value of P is 86.2 kN or 84% of the ACI value.

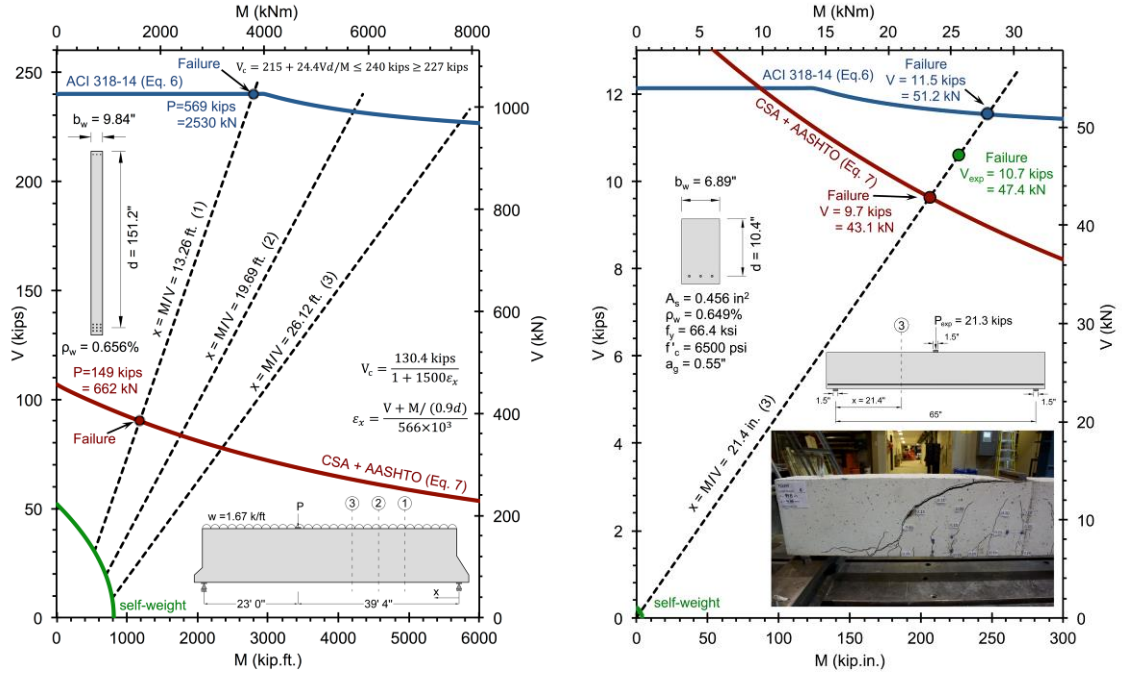


(a) PLS4000 (b) PLS300

Figure 6. Predicted shear failure loads of 4 m thick and 300 mm thick slab strips

## LOADING TO FAILURE OF EAST SHEAR SPAN PLS4000

Specimens PLS4000 and PLS300 were cast on April 27th 2015 and loading of PLS4000 began on June 10th 2015 using a displacement controlled actuator. Figure 7 is the recording from the X-Y plotter used to control the experiment. The plotter shows the relationship between the magnitudes of the applied point load on the Y axis against the deflection measured by an LVDT directly below the point load. Three University of Toronto professors made load-deformation predictions and these were plotted on the graph paper prior to starting the test. First flexural cracking was observed at P = 198 kN and full load stages were taken at 250 kN, 325, 500 and 625 kN. At each load stage, the load was reduced somewhat to ensure safety of the students

marking cracks and measuring crack widths. At the end of each day of testing the load was reduced to zero overnight. The other reductions in load on the graph were caused by the formation of major new cracks. As the point load reached its maximum value of 685 kN (a value just 4% higher than the MCFT prediction) a flexural crack about 5.5 m from the east support began to spread upwards, crossed mid-depth with a slope of about 45° and as it propagated towards the point load the force applied by the displacement controlled jack reduced to less than 500 kN indicating a typical shear failure. At 5.5 m from the east support the shear at the peak load was 97.6 + 685 x 7/19 = 350 kN. After the peak load Load Stage 5 was taken and crack widths at mid-depth were found to be up to 3 mm wide. At this stage the photograph in Fig. 2 was taken. After the weekend the damaged specimen was reloaded and reached a maximum load of only 433 kN at which load the cracks spread and widened and the point load reduced to just 13 kN. Load Stage 6 was taken at this stage, see Fig.8, with crack widths being up to 35 mm wide.

Note from Fig.8 that in the east shear span there are three visible cracks which cross over mid-depth of the large specimen and the horizontal spacings between these three cracks are 0.68 d and 0.59 d. For the companion small specimen the spacings between the three cracks that cross over mid-depth, see Fig.6 (b), are 0.73 d and 0.50 d. Thus as the depth d goes up by a factor of 14.5, the crack spacing at mid-depth goes up by about the same ratio resulting in much wider cracks in the larger member for the same tensile strain in the longitudinal reinforcement. This is the prime reason for the size effect in shear.

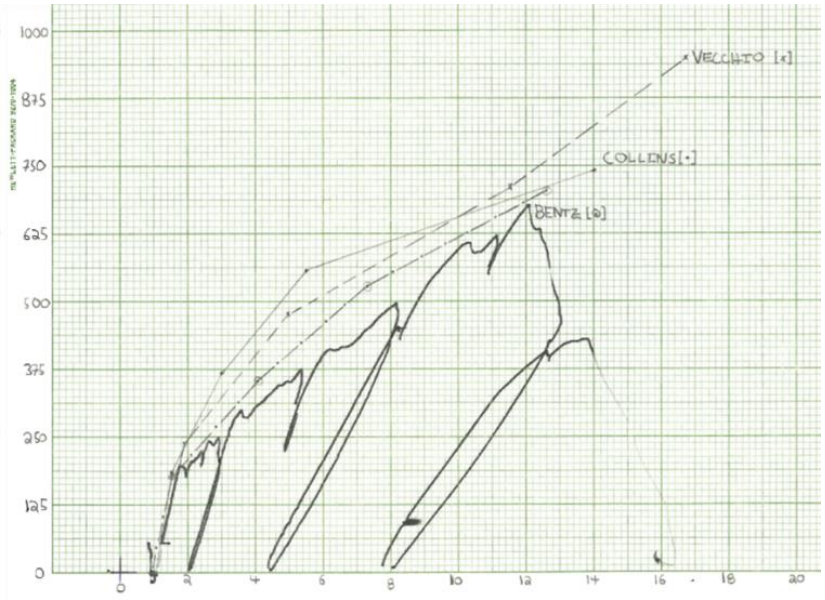


Figure 7. Load-deflection response of PLS4000 east

Figure 8. East span of PLS4000 after failure

## LOADING TO FAILURE OF WEST SHEAR SPAN OF PLS4000

In order to determine the shear capacity of the shorter west shear span which contained shear reinforcement the failed east end of the specimen was repaired by strapping that shear span with four pairs of 36 mm diameter post-tensioned Dywidag threadbars. The point load was then increased and the resulting load-deformation response is shown in Fig. 9. Load stages were taken when the point load reached 1000 kN, 1375 kN, 1750 kN and 2020 kN and failure occurred with crushing of the concrete near the loading plate when P reached 2162 kN, see Fig. 10.

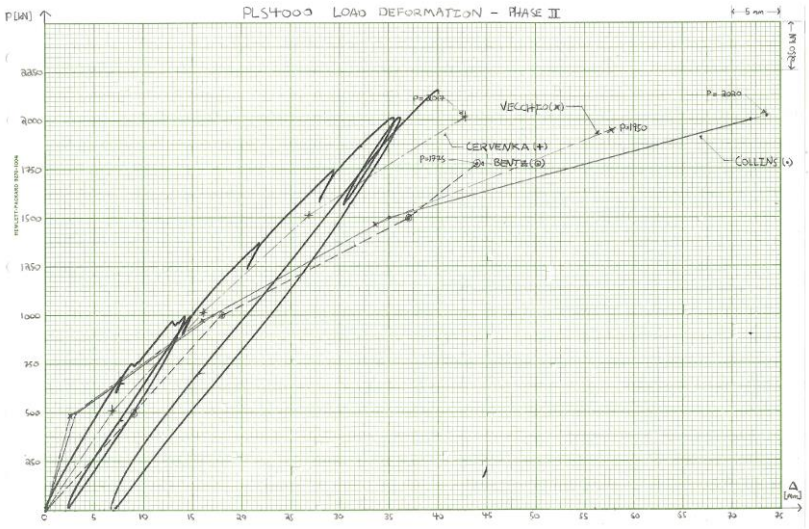


Figure 9. Load-deflection response of PLS4000 west

Figure 10. Specimen PLS4000 after failure of short shear span with shear reinforcement

Note that the shear force required to fail the shorter west shear span with widely spaced minimum shear reinforcement was 146 + 2162 x 12/19 = 1512 kN which is 1512/350 = 4.3 times the magnitude of the failure shear of the longer east shear span with no shear reinforcement.

## PREDICTIONS SUBMITTED BY ENGINEERS

Figure 11 (a) compares the experimental result from the east shear span with the 66 predictions made by engineers who responded to the challenge of predicting the failure load of the very thick slab. Also shown on the plot are the predictions made by six different codes. Given the large range of values shown in the figure and the almost uniform distribution of predicted values across the entire range it is evident that predicting the shear strength of very thick slabs not containing shear reinforcement was a challenging task for the profession. The upper “red” zone in the figure identifies very unconservative predictions where the ratio of

predicted failure load to observed failure load goes from 1.5 to 5.5. The “yellow” band in the figure, on the other hand, indicates the “gold standard” prediction range of plus or minus 10% from the observed strength. It can be seen that based on this measure, eight of the predictions from industry, five from academia and three predictions from codes were excellent. While 20% of the entries were very accurate, the concern is that 44% of the entries and two of the codes were in the red zone and thus made very unconservative predictions.

Figure 11(b) compares the experimental value of the point load required to fail the west shear span with the 44 predictions made by engineers who responded to the challenge of predicting the failure load of the specimen if the east shear span had also contained shear reinforcement. Comparing Fig. 11(a) and (b) it can be seen that while 29 of the 66 entries were in the red zone for the east shear span without shear reinforcement, for the west shear span only one of the 44 entries was in the red zone. Further for the west shear span 66% of the predictions were conservative while for the east shear span only 24% were conservative. For the west shear span ten of the predictions, five from industry, four from academia and the ACI value were within 10% of the experimental value.

There are two CSA predictions shown in Fig.11 one based on sectional analysis, Eq. (1), and the second on a strut-and-tie (S&T) analysis. For this specimen the strut-and-tie estimate of failure was only 11% higher than the sectional value indicating that strut action while significant is not yet as dominant as it would be for a somewhat shorter shear span.

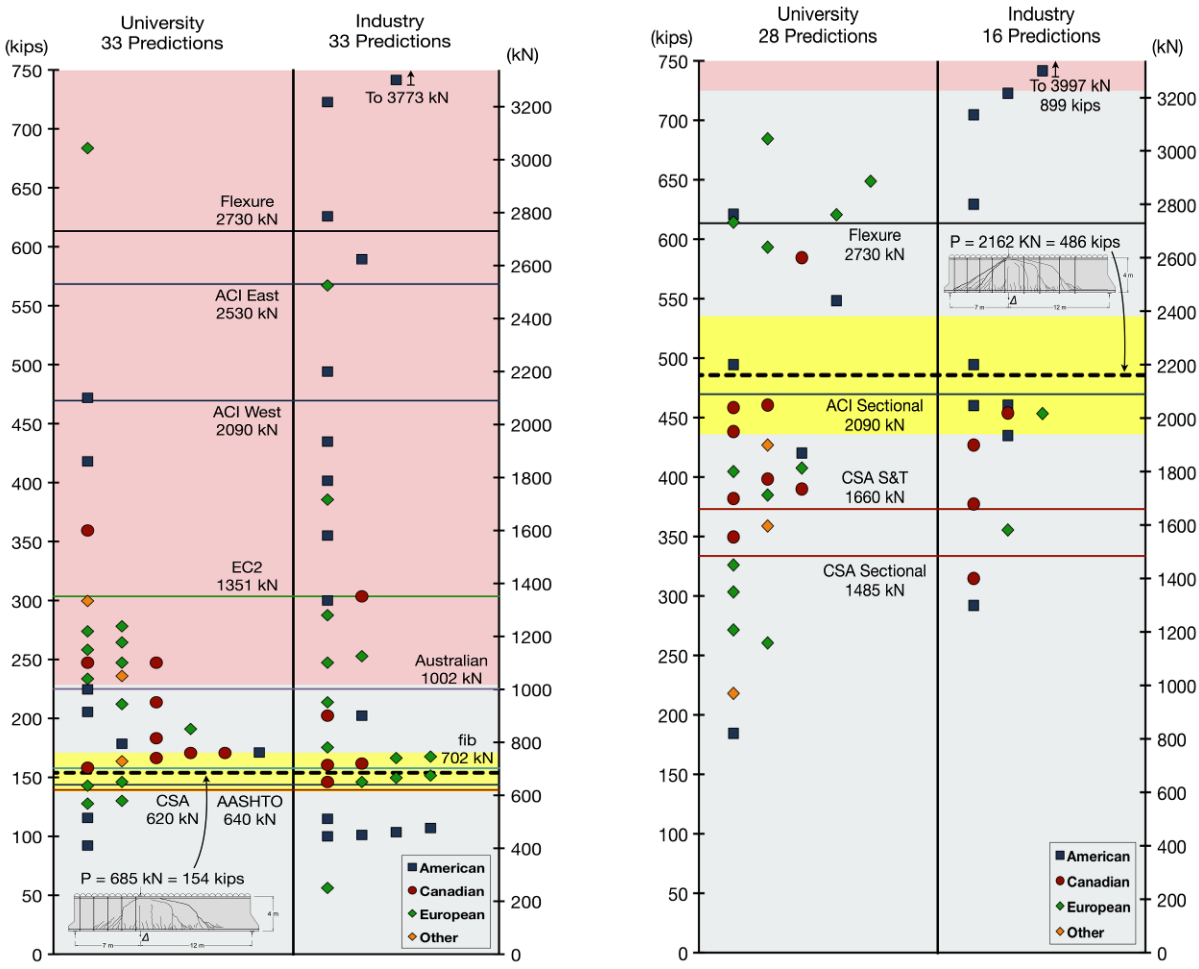


(a) East Shear Span

(b) West Shear Span

Figure 11. Comparisons of predictions of point load P to cause failure with test results

## THE TORONTO SIZE EFFECT SERIES FOR MEMBERS IN SHEAR

In designing the large slab strip specimen and its companion small specimen the shear span to depth ratio, a/d, the percentage of longitudinal reinforcement and the concrete strength were chosen so that the new specimens would be compatible with previous tests at Toronto investigating the size effect in shear (Collins and Kuchma 1999, Lubell et al 2004, Sherwood et al 2010). The eleven specimens with the similar properties are described in Table 1 and the experimental results are compared with the ACI and MCFT predictions in Fig. 12. It is interesting to note how well the MCFT predictions match the experimental results over the member size range where the largest specimen is 35 times as big as the smallest specimen.

Table 1. Properties of specimens in Toronto size effect series.

| Name | fc' MPa | $a_g$ mm | $\rho$ % | a/d | $b_w$ mm | d mm | $V_{exp}$ kN | $V_{exp}$ kN/m | $v_{exp}$ MPa | $v_{mcft}$ MPa | $\frac{v_{exp}}{v_{mcft}}$ |
|---|---|---|---|---|---|---|---|---|---|---|---|
| BN12 | 37.2 | 10 | 0.91 | 3.1 | 300 | 110 | 40 | 133 | 1.347 | 1.136 | 1.19 |
| BN25 | 37.2 | 10 | 0.89 | 3.0 | 300 | 225 | 73 | 243 | 1.202 | 1.058 | 1.14 |
| PLS300 | 44.8 | 14 | 0.65 | 3.1 | 175 | 264 | 47.4 | 271 | 1.140 | 1.037 | 1.10 |
| S-10N1 | 41.9 | 10 | 0.83 | 2.9 | 122 | 280 | 36.6 | 300 | 1.190 | 1.048 | 1.14 |
| S-10N2 | 41.9 | 10 | 0.83 | 2.9 | 122 | 280 | 38.3 | 314 | 1.246 | 1.048 | 1.19 |
| BN50 | 37.2 | 10 | 0.81 | 3.0 | 300 | 450 | 132 | 440 | 1.086 | 1.026 | 1.06 |
| BN100 | 37.2 | 10 | 0.76 | 2.9 | 300 | 925 | 192 | 640 | 0.769 | 0.721 | 1.07 |
| L-10N1 | 38.4 | 10 | 0.83 | 2.9 | 300 | 1400 | 265 | 883 | 0.631 | 0.636 | 0.99 |
| L-10N2 | 40.3 | 10 | 0.83 | 2.9 | 300 | 1400 | 242 | 807 | 0.576 | 0.647 | 0.89 |
| YB2000/0 | 33.6 | 10 | 0.74 | 2.9 | 300 | 1890 | 281 | 936 | 0.551 | 0.510 | 1.08 |
| PLS4000 | 40.0 | 14 | 0.66 | 3.1 | 250 | 3840 | 350 | 1400 | 0.405 | 0.381 | 1.06 |

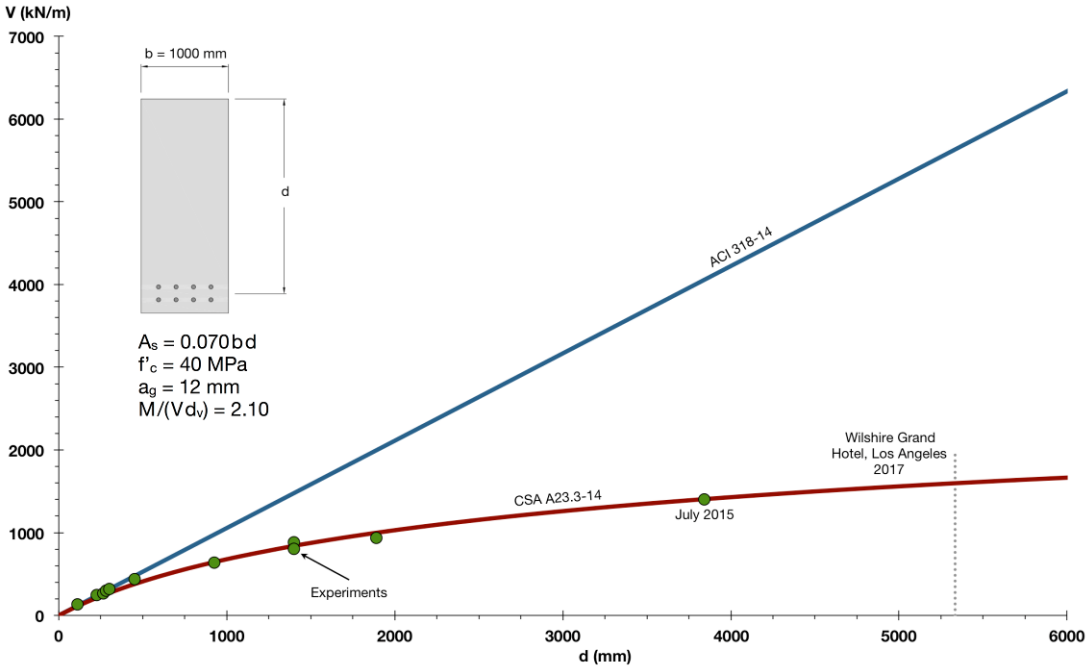


Figure 12. The size effect in shear for members without shear reinforcement

## HEAVILY REINFORCED COUPLING BEAMS

In the design of high-rise residential buildings minimizing storey-to-storey height typically improves the economy of the building. Because of this the coupling beams of the shear walls of such buildings are often made from high strength concrete and are very heavily reinforced so that their depth can be minimized. There is concern that for such members the cover concrete may spall as failure approaches reducing the effective width of the beam. To investigate these concerns four full scale heavily reinforced coupling beams are to be tested to failure, with the completion of the first of these experiments, CBF1, being shown in Fig. 13. The properties of the four beams are given in Fig. 14. Note that three of the beams exceed the maximum amount of shear reinforcement permitted by the ACI code.


Figure 13. Specimen CBF1 after failure, $V_{max}$ = 1918 kN, right wall pushed down 70 mm.

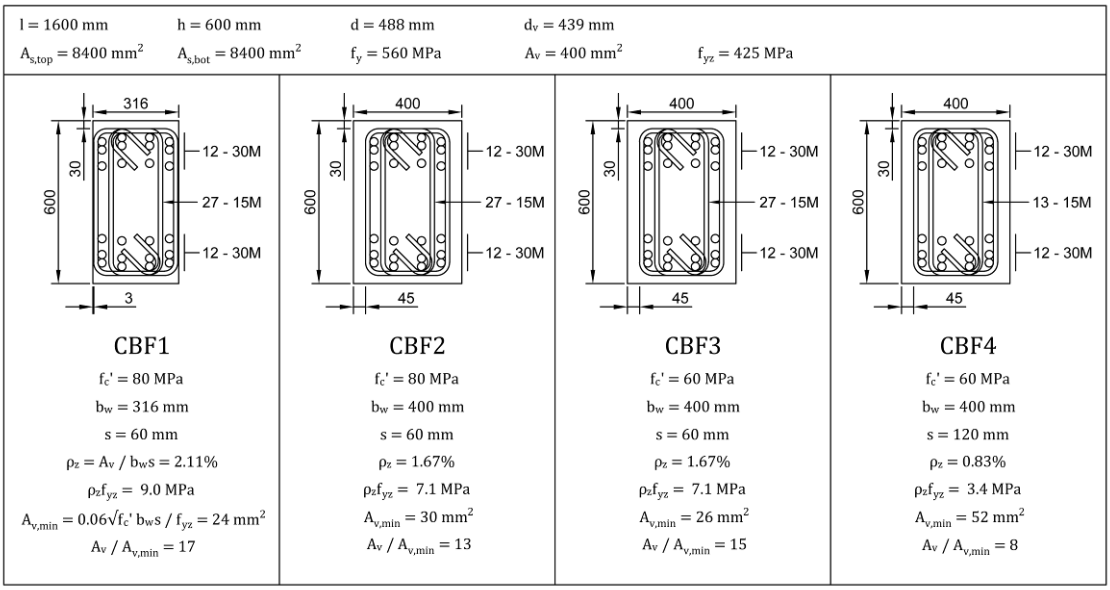


Figure 14. Properties of the four coupling beams, the ACI code limits $A_v/A_{v,min}$ to 11

The ACI code has traditionally limited the shear capacity of a reinforced concrete section to 10 $\sqrt{f_c'}$ $b_w d$ with an upper limit of 1000 $b_w d$ (psi units). For CBF1 this upper limit corresponds to a shear force of 1064 kN or just 56% of the experimental failure shear. The simplified MCFT of Eq. (1) on the other hand predicts a failure shear of 1840 kN or 96% of the experimental failure load. Program Membrane using the full MCFT predicts that the failure shear at mid-span of the coupling beam, where M=0, will be 1940 kN while program Response predicts 1949 kN. The experimental load-deformation is compared with the predictions from these two MCFT programs in Fig. 15. Note that the Membrane prediction includes only the deformation due to shear strain. The wall displacement measuring rod, crack widths and concrete splitting and spalling near peak load are shown in Fig. 16. Post peak the beam continued to resist substantial shear as the deformation increased.

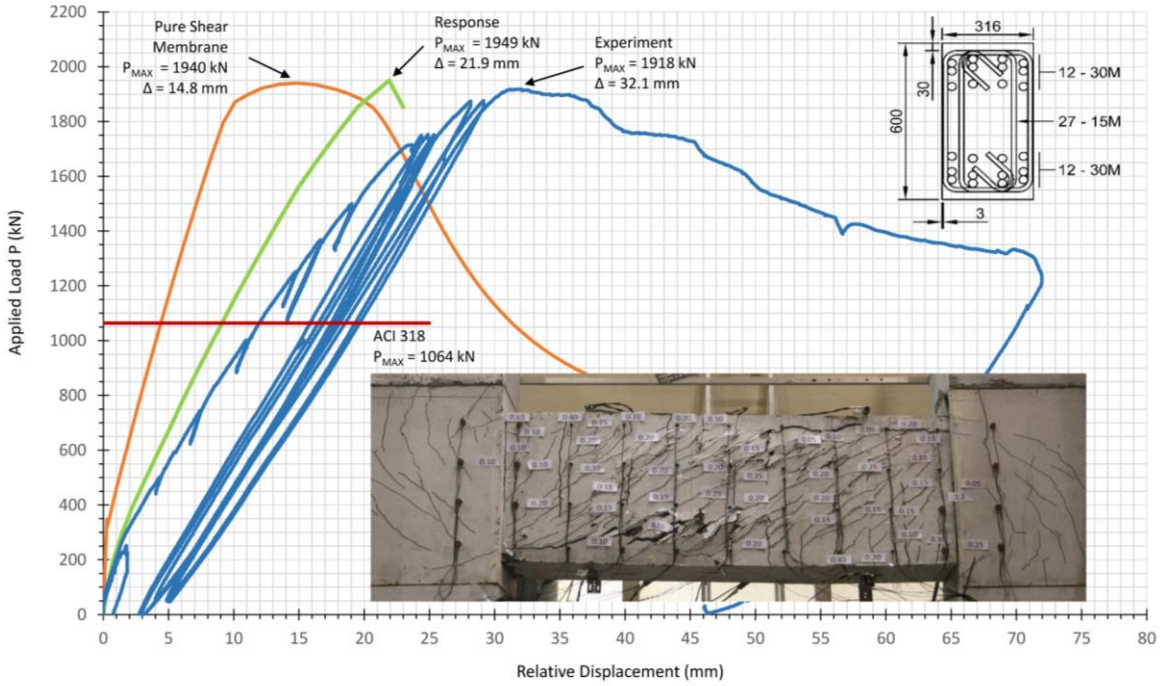


Figure 15. Observed and predicted load-deformation response of CBF1

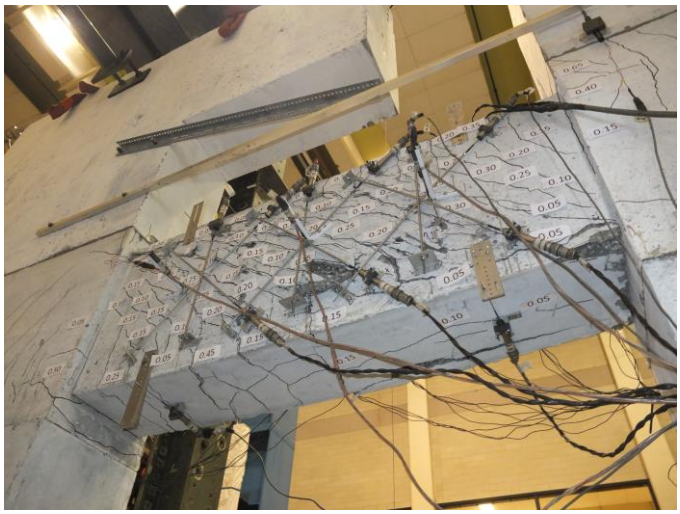

Figure 16. Instrumentation on back face, wall-to-wall displacement rod.

## CONCLUDING REMARKS

This paper has summarized the shear design procedures developed at the University of Toronto over the past 40 years. These procedures are based on the Modified Compression Field Theory (MCFT) which is capable of predicting accurately the shear behaviour of cracked reinforced concrete under general biaxial loading conditions. In addition the paper has described two current research projects one involving testing to failure of a strip from a four metre thick slab and the other involving loading full-scale coupling beams of shear walls. The paper has summarized the 2014 Canadian shear provisions based on the MCFT and shown how they can be used to calculate the shear strength for a wide variety of members and structures.

To investigate the ability of current design procedures to predict the shear strength of very thick slabs engineers were invited to predict the magnitude of the point loads required to fail the two shear spans. The shear strength of the longer shear span with no shear reinforcement of the very thick slab was dangerously overestimated by many engineers resulting in 44% of the 66 entries predicting failure loads more than 1.5 times the experimental values and 12% submitting predictions more than three times the experimental value. The ACI 318-14 prediction, which ignores the size effect, was 3.7 times the experimental value while EC2 (which underestimates the size effect) predicted 2.0 times the experimental value. It is concluded that these two influential shear design procedures can seriously overestimate the strength of very thick slabs in long shear spans not containing shear reinforcement. The second and more positive conclusion is that, as shown by 20% of the entries and three of the codes, excellent estimates of failure load for such shear spans can be made. The third and perhaps most important conclusion is that adding minimum shear reinforcement essentially eliminates the size effect in shear and so greatly increases the shear strength of very thick slabs.

While predicted flexural capacities given by different internationally respected design codes agree very closely, the predicted shear capacities may differ by factors as high as three. The difficulty is that shear strength is influenced by many more parameters than flexural strength and most laboratory experiments have been conducted on rather small specimens with a rather narrow range of parameters. Because of this, the traditional empirically-based shear provisions can give unsafe predictions when applied to large, lightly-reinforced members or to members made with new materials such as high strength concrete, self compacting concrete, FRP reinforced concrete or members reinforced with high strength steel.

Given the large number of existing concrete structures designed using shear provisions now known to be unconservative, and the limited resources available to increase public safety, it is essential that the shear design procedures used to evaluate these structures be as accurate as possible. In ranking structures most in need of repair it is equally problematic to have design methods that for some structures are excessively conservative, such as the ACI estimate for the coupling beam, as it is to have methods that are for some structures dangerously unconservative, such as the EC2 predictions for the thick slab. Currently shear provisions based on the MCFT provide the most accurate estimates of shear capacity. The low scatter demonstrated by these provisions is despite, or, perhaps, because of the fact that these shear provisions are theoretically based, rather than being fitted to the experimental database. It is hoped that the methods presented in this paper will allow better allocation of resources to structures that are most in need of repair.

## REFERENCES


AASHTO, (2012), "LRFD Bridge Design Specifications and Commentary", 6th Edition, American Association of State Highway Transportation Officials, Washington, 2012, 1264 pp.
ACI Committee 318, (2014), "Building Code Requirements for Structural Building (ACI 318-14) and Commentary," American Concrete Institute, Farmington Hills, MI, 2014, 519 pp.

ACI-ASCE Committee 326, (1962), "Shear and Diagonal Tension," *ACI Journal, Proceedings*, V.59, No.1, 2, and 3, Jan., Feb., and Mar., 1962, pp. 1-30, 277-334, and 352-396 and discussion and closure, Oct 1962 pp. 1323-1349.

Bentz, E.C. and Collins, M.P., (2006), "Development of the 2004 CSA A23.3 Shear Provisions for Reinforced Concrete", Canadian Journal of Civil Engineering, V. 33(5), pp. 521-534

Bentz, E.C. (2014), http://www.ecf.utoronto.ca/~bentz/m2k.htm, Membrane webpage last accessed 2014/02/13

Bentz, E.C. (2014), http://www.ecf.utoronto.ca/~bentz/r2k.htm, Response webpage last accessed 2014/02/13

Collins, M.P., (1978), "Towards a Rational Theory for Reinforced Concrete Members in Shear," Journal of the Structural Division, ASCE, 104(4), pp. 649-666.

Collins, M.P. and Kuchma, D., (1999), "How Safe Are Our Large, Lightly Reinforced Concrete Beams, Slabs and Footings?", ACI Structural Journal V. 96, No. 4, July-August, pp. 482-490.

CSA Technical Committee on Reinforced Concrete Design,(2014), "CSA A23.3-14 Design of Concrete Structures", Canadian Standards Association, Mississauga, Ontario, Canada, 290 pp.

European Committee for Standardization, (2004), CEN, EN 1992-1-1:2004 Eurocode 2: "Design of Concrete Structures- Part 1-1: General rules and rules for buildings", Brussels, Belgium, 225 pp.

International Federation For Structural Concrete (fib), (2013), "fib Model Code for Concrete Structures 2010," Ernst & Sohn, Lausanne Switzerland, 402 pp.

Lubell, A.S., Sherwood, E.G., Bentz, E.C. and Collins, M.P., (2004), "Safe Shear Design of Large, Wide Beams", ACI Concrete International, V.26, No. 1, pp. 66-78.

Nieblas, G.M., (2014), "Reaching New Heights in Los Angeles", STRUCTURE magazine, NCSEA, http://www.structuremag.org/?p=7818

Sherwood, E.G., Bentz, E.C. and Collins, M.P., (2007), "Effect of Aggregate Size on Beam-Shear Strength of Thick Slabs", *ACI Structural Journal,* Vol. 104, No. 2, March-April 2, pp. 180-190.

Vecchio, F. J. and Collins, M. P.,(1986), "The Modified Compression-Field Theory for Reinforced Concrete Elements Subjected to Shear", *ACI Structural Journal*, Vol. 83, No. 2, Mar.-Apr., pp. 219-231.

Vecchio, F.J., (2014), http://www.civ.utoronto.ca/vector , VecTor2 webpage, last accessed 2014/02/13

Walraven, J.C., (1981), "Fundamental Analysis of Aggregate Interlock," Journal of the Structural Division, ASCE, 107(ST11), pp 2245-2270.